Nuclear Engineering and Technology 53 (2021) 894–900

Contents lists available at ScienceDirect

Nuclear Engineering and Technology

journal homepage: www.elsevier.com/locate/net

Original Article

Sorption of Pd on illite, MX-80 bentonite and shale in Na–Ca–Cl solutions

Jared Goguen [2], [*], Andrew Walker, Joshua Racette, Justin Riddoch [1], Shinya Nagasaki

Engineering Physics, McMaster University, 1280 Main Street West, Hamilton, L8S 4L7, Canada

ARTICLE INFO

Article history:
Received 8 January 2019
Received in revised form
1 September 2020
Accepted 2 September 2020
Available online 9 September 2020

Keywords:
Sorption
Sorption distribution coefficient
2SPNE SC/CE model
PHREEQC
Geological disposal
Palladium

ABSTRACT

This paper examines sorption of Pd(II) onto illite, MX-80 bentonite, and Queenston shale in Na–Ca–Cl solutions of varying ionic strength (IS) from 0.01 to 6.0 mol/L (M) and pH_c ranging from 3 to 9 under atmospheric conditions. A 2-site protolysis non-electrostatic surface complexation and cation exchange model was applied to the Pd sorption onto illite and MX-80 using PHREEQC, and the model results were compared to the experimental ones obtained in this work. Surface complexation and cation exchange constants were estimated for both illite and MX-80 through the optimization process to bring the predicted distribution coefficients from the model into alignment with the experimentally derived values. These optimized surface complexation constants were compared to existing linear free energy relationships (LFER).

1. Introduction

Deep geological repositories (DGRs) are being considered for the long-term management of nuclear waste in Ontario, Canada under the Nuclear Waste Management Organization's (NWMO) Adaptive Phased Management (APM) strategy. Potential sites for these DGRs contain natural geological barriers that consist of argillaceous limestone and shale. Additionally, highly compacted bentonite clay blocks are being considered as an engineered barrier for encasement of the used-fuel container and backfill of the site [1]. The NWMO is designing the DGRs for millions of years of containment, requiring the conducting of comprehensive safety analyses before licensing sites for operation [2]. Part of the safety assessment uses mathematical models to represent the diffusion and migration of radionuclides through the geosphere. These models heavily rely on robust surface complexation models (SCMs). Some of the integral components of the SCMs are the sorption mechanisms and characteristics of the nuclides in the ground and pore waters. In Ontario, the ground and pore waters at the DGR depths were found to have an ionic strength (IS) as high as 7.2 M, which could affect sorption [3].

Palladium is selected as an element of interest by the NWMO due to the long half-life of Pd-107 (6.5×10^6 a) and its significant presence in the non-uranium components of used nuclear fuel. Pd is expected to exist in the +II redox state in the ground waters of Ontario [4]. Previous studies on Pd sorption have been conducted under different conditions for different applications. Batch sorption of K_2PdCl_4 and $Cu(NO_3)_2$ in deionized water (DI) solutions onto bentonite from Gorbskoye (Trans-Carpathian region) and Dashukovskoye (Cherkassy region) deposits in Ukraine was studied by Rakitskaya et al. [5] to determine how bentonite origin can affect catalytic activity of the supported metal complexes in the reaction of CO oxidation with O_2 contained in air (most affected by the formation mechanism and bond strength). It was concluded that competitive adsorption takes place between K_2PdCl_4 and $Cu(NO_3)_2$, and that the adsorption sites between the two bentonite samples were not homogeneous [5]. Kinetics and isotherm experiments have been conducted from 18 °C–40 °C for Pd batch sorption onto Diaion WA21J anionic exchange resin in Cl solutions [6]. Batch kinetics and isotherm experiments for Pd adsorption onto hybrid montmorillonite and Laponite–calcium alginate gel beads have also been conducted in DI and NaCl solutions (IS = 0.01 M) in the acidic pH region (pH = 2–4). Langmuir and Freundlich isotherms were fit to the experimental adsorption data and showed that the

* Corresponding author.
E-mail address: Jared.Goguen@brucepower.com (J. Goguen).
[1] Present address: Ontario Power Generation, 1675 Montgomery Park Road, Pickering, ON, L1R 2V5, Canada.
[2] Present address: Bruce Power, 177 Tie Rd, Tiverton, ON, N0G 2T0, Canada.

https://doi.org/10.1016/j.net.2020.09.001
1738-5733/

addition of the clay minerals to the alginate gel beads increased Pd adsorption by more than 50% [7]. Batch sorption experiments of Pd on pumice tuff with different NH_3 and NH_4^+ concentrations, solution pH, and IS have also been performed, and it was found that Pd sorption decreased with an increase in the concentration of NH_4^+, suggesting the formation of stable ammine complexes ($Pd(NH_3)_m^{+2}$) for initial concentrations of NH_4^+ greater than 10^{-4} M [8]. The only existing relevant sorption data for Pd consists of a set of 24 data points for bentonite in 0.01 and 0.1 M NaCl solutions [9], which is not a high enough IS to replicate the conditions in potential DGR sites in Ontario, and does not contain calcium as outlined in the NWMO reference pore water for sedimentary rock [3]. To fill this requirement, sorption of Pd onto Queenston shale, illite (the major clay constituent of shale), and MX-80 bentonite (the engineered barrier for the highly compacted bentonite blocks and backfill) in Na–Ca–Cl solutions with IS ranging from 0.01 to 6.0 M and pH_c (molar H^+ concentration) ranging from 3 to 9 are examined in this paper.

In order to develop a more detailed understanding of the sorption process, sorption for a given element, across the pH spectrum and in solutions of varying IS, needs to be modelled and correlated to the experimental data. Once the processes by which sorption occurs are determined, modelling those processes allows for the determination of the equilibrium constants of the various sorption reactions (Log K). Establishing the reaction constants for the various sorption processes allows for the accurate prediction of sorption in varying conditions over time and space, which can be used to improve the migration models in the post-closure safety assessments. A common geochemical code used for modelling sorption is PHREEQC, which stands for PH REdox EQuilibrium in the language C [10]. The model in PHREEQC makes use of a thermodynamic database (TDB), as a source of reference values, in order to make all of the necessary calculations. Reactions considered in the model can be derived from those in Ref. [11].

The 2-site protolysis non-electrostatic surface complexation and cation exchange (2SPNE SC/CE) model has been successfully applied to simulate the sorption of Mn(II), Co(II), Cd(II), Ni(II), Zn(II), Fe(II), Eu(III), Am(III), Sn(IV), Th(IV), Np(IV), Np(V), U(VI), Pa(V) onto illite and montmorillonite [12–18]. In this paper, we applied the 2SPNE SC/CE model to experimentally derived R_d values of Pd on illite and MX-80 and estimated the optimized equilibrium constants of sorption reactions.

2. Experimental

2.1. Chemicals & instrumentation

All chemicals used were reagent grade and supplied from Fisher Scientific. Deionized water was supplied from a Milli-Q Direct 8. All Pd used in experiments was derived from a 1000 ± 1 μg/mL stock solution with a natural isotopic abundance, and all concentration measurements were conducted with a Triple Quad 8800 inductively coupled plasma mass spectrometer (ICP-MS): both obtained from Agilent Technologies. The Pd initial concentration (C_i) used in the sorption experiments was set to 1.0×10^{-7} M, which was confirmed to be lower than the solubility in Na–Ca–Cl solutions of IS = 0.1–6 M (Fig. A1 in the Supplemental Information).

Saline solutions (IS = 0.01–6 M) were prepared with the combination of NaCl, $CaCl_2 \cdot 2H_2O$, and DI, while maintaining the same 2.7 Na/Ca molar ratio as that defined in the reference brine water proposed by the NWMO [3]. Masses were all measured using a Sartorius Quintix 213-1S.

Three solids were used in the sorption experiments: IMt-2 Na-illite from Silver Hill, USA (acquired from the Clay Mineral Society), Volclay MX-80 Na-bentonite from Wyoming, USA (acquired from the American Colloid Company (ACC)), and Ordovician-age Queenston shale from Ontario, Canada (provided by the NWMO). The illite and shale core samples were manually crushed and sieved to a grain size between 150 and 300 μm, and MX-80 was specified by the ACC to contain grain sizes ranging from 74 to 420 μm and was used as received [19].

The pH values observed on the pH meter (pH_{obs}) should be considered as operational values [20]. The relationship between pH_{obs} and the molar H^+ concentration ($pH_c = -\log c_{H+}$) or the molal H^+ concentration ($pH_m = -\log m_{H+}$) were discussed in detail by Altmaier et al. [21,22]. In this study, the relationship between pH_{obs} (measured with a VWR 89231-590 dual junction Ag/AgCl$_2$ electrode and a VWR B10P symphony benchtop meter) and pH_c in solutions was determined by acid-base titration (Metrohm Ti-Touch 916) in desired media, and the pH_{obs} values were converted to the pH_c values.

2.2. Sorption procedure

All sorption experiments were carried out at 25 °C in triplicate under atmospheric conditions. Preliminary tests were performed to confirm that sorption of Pd to the wall of the reaction vessel was negligible. Since the basic procedures of sorption experiments were the same as those we used in the sorption experiments of Np(V) and Np(IV) [16,23], only the differences in the procedure and conditions from the previous ones are described in this paper.

The liquid/solid ratio for all samples was 0.50 ± 0.02 m^3/kg, resulting from 8.00 ± 0.05 mL of solution and 16.0 ± 0.5 mg of sorbent. Aliquots of each Pd sample were removed from sorption test tubes after 14 days and placed in Nalgene centrifuge containers for centrifugation at 18,000 rpm for 30 min. We previously confirmed that the liquid phase was sufficiently separated from the solid phase by this method [19]. Supernatants were diluted with DI to ensure that the solution salinity was below 0.75 M before concentration measurements were taken, as required by the ICP-MS [24].

The primary measure of sorption is called the sorption distribution coefficient (R_d) (m^3/kg), which is calculated according to Eq. (1), where C_i is the initial concentration of Pd in solution (1.0×10^{-7} M), C_{eq} the equilibrium concentration post-sorption (M), L the volume of liquid used in the sample (m^3), and m the mass of solid used (kg).

$$R_d = \frac{C_i - C_{eq}}{C_{eq}} \times \frac{L}{m} \tag{1}$$

2.2.1. Sorption kinetics

To determine sorption duration, sorption kinetics tests were conducted in sample solutions with IS = 0.1, 1.0, and 4.0 M for all three sorbents. Test samples had a C_i of $(1.0 \pm 0.05) \times 10^{-7}$ M, and concentrations were measured 1 h, and 1, 2, 5, 7, and 14 days after contacting the sorbent. The pH_c values were not adjusted but were found to have been between 5.3 and 5.6, 5.8–6.6, and 6.3–7.4 during the kinetics test periods for illite, MX-80, and shale, respectively.

2.2.2. Ionic strength dependence

The dependence of Pd sorption on solution salinity was determined for all three sorbents at IS = 0.1, 0.5, 1.0, 2.0, 3.0, 4.0, 5.0, and 6.0 M. The pH_c values were not adjusted but were found to have been between 5.4 and 5.8, 6.0–6.9, and 6.5–7.7 during the sorption test periods for illite, MX-80, and shale, respectively.

2.2.3. pH_c dependence

A separate set of experiments was conducted in order to determine the dependence of Pd sorption on pH_c for all three sorbents. For illite and MX-80, sorption tests were conducted at pH_c = 3.0, 4.0, 5.0, 6.0, 7.0, 8.0, and 9.0 at each of the following solution salinities: 0.01, 0.1, 1.0, 4.0, and 6.0 M. For shale, sorption tests were conducted at pH_c = 5.0, 6.0, 7.0, 8.0, and 9.0 at each of the following solution salinities: 0.1, 1.0, 4.0, and 6.0 M. The pH_c was adjusted using 0.1 N HCl and NaOH. The pH_c of the solution was measured once a day and re-adjusted to the original pH_c value if the pH_c changed by more than ±0.2 from the original value.

3. Model

The pH_c dependence of Pd R_d values for illite and MX-80 was fitted using a 2SPNE SC/CE model with the geochemical code PHREEQC. The LFERs this model is based on were developed for illite and montmorillonite [12–14]; however, MX-80 is comprised of approximately 80% montmorillonite [3]. Therefore, the MX-80 data was modelled using a montmorillonite analogue. The specific-ion interaction theory (SIT) was used for the computational method, as it accounts for the electrostatic interactions of all other ions in solution with the one ion of interest. This is necessary for accuracy when computing activity coefficients in solutions of high IS, as these interacting electrostatic forces assert a greater influence. The Pitzer computational method can be more accurate in very high IS solutions; however, Pitzer parameters for Pd were not known at the time of this study. SIT is not known to be accurate above an IS of 4.0 M [25] and, therefore, sorption was modelled at IS ≤ 4.0 M in this study. The solutions modelled had the same IS and Na–Ca–Cl concentrations as those used in the experiments. Solutions containing Pd had C_i values equal to that of the experimental conditions: 1.0×10^{-7} M.

3.1. Thermodynamic data

The Japan Atomic Energy Agency (JAEA) thermodynamic database (TDB) was chosen as the reference database since it contains the necessary thermodynamic data for Pd [26]. Formation reactions for the relevant Pd aqueous species and their constants contained in the JAEA TDB are shown with their listed errors in Table 1. No formation reaction constants (FRCs) were contained in the database for the $PdOH^+$ and $Pd(OH)_4^{2-}$ aqueous species, so the values contained in the SIT database (v9a) included in the PHREEQC download package [27] were added to the JAEA TDB.

Surface hydroxyl groups can behave as an acid or base and have associated clay-specific reaction constants, called protolysis reaction constants, for both protonation and deprotonation. These constants for strong ($\mathrm{Log}^{S}K$) and weak ($\mathrm{Log}^{W}K$) surface sites were obtained from Bradbury and Baeyens [12–14]. Cation exchange was included in the model to help improve the sorption predictions in low IS and low pH_c conditions. The selectivity coefficients (Log K_c) for H^+ and Ca^{2+} were obtained from Bradbury and Baeyens [13] for illite, having values of 0.0 and 1.04, respectively. These coefficients were obtained from Charlet and Tournassat [28] for MX-80, having values of 0.0 and 0.5, respectively.

Table 1
Formation reactions of relevant Pd(II) species.

Formation Reaction	Log K	Error	Reference
$Pd^{2+} + H_2O{-}H^+ \leftrightarrow PdOH^+$	−1.86	0.29	[27]
$Pd^{2+} + 2H_2O{-}2H^+ \leftrightarrow Pd(OH)_2$	−3.49	–	[26]
$Pd^{2+} + 3H_2O{-}3H^+ \leftrightarrow Pd(OH)_3^-$	−15.48	0.35	[26]
$Pd^{2+} + 4H_2O{-}4H^+ \leftrightarrow Pd(OH)_4^{2-}$	−29.36	–	[27]
$Pd^{2+} + Cl^- \leftrightarrow PdCl^+$	5.00	0.24	[26]
$Pd^{2+} + 2Cl^- \leftrightarrow PdCl_2$	8.42	0.31	[26]
$Pd^{2+} + 3Cl^- \leftrightarrow PdCl_3^-$	10.93	0.38	[26]
$Pd^{2+} + 4Cl^- \leftrightarrow PdCl_4^{2-}$	13.05	0.59	[26]
$Pd^{2+} + 3Cl^- + H_2O{-}H^+ \leftrightarrow PdCl_3OH^{2-}$	3.77	0.63	[26]

3.2. Surface properties

The quantitative sorbent properties required to be defined in PHREEQC include the total mass of solid (g), number of surface sites (moles), and the specific surface area (SSA) (m^2/g). The product between solid mass and surface site capacity (density) yields the total number of surface sites. Site capacities of 2.0×10^{-3} mol/kg for strong sites ($S^{S}OH$) and 4.0×10^{-2} mol/kg for weak sites ($S^{W}OH$), for both clays, were obtained from Bradbury and Baeyens [12,14], which were used to calculate the total number of surface sites used in the model. Given the trace concentration of Pd used in the experiments, strong sites should be dominant in the sorption process and weak sites should not significantly contribute [3]. Furthermore, the LFER for illite only includes strong sites [14]. Therefore, only strong sites were used in the sorption model for Pd.

The illite used in this work was collected from Silver Hill in Montana, USA, and has a SSA of 70 m^2/g [29]. When developing the LFER, sorption tests were conducted on illite samples collected from the Le Puyen-en-Velay (Haute-Loire) region of France, which have a SSA of 97 m^2/g [13,14]. In order to make use of the LFER developed by Bradbury and Baeyens for illite [13,14], and to make direct comparisons to the proposed sorption reaction constants for illite based on samples from France, an adjustment had to be made to the total number of sites in the model by a factor of 70/97. The SSA used for MX-80 was 26.2 m^2/g, which was obtained from Bertetti [30]. Ion-exchange capacities of 21 meq/100 g and 102.1 meq/100 g were obtained from Pivovarov et al. [29] for illite and Villa-Alfageme et al. [31] for MX-80, respectively.

3.3. Sorption

The initial surface complexation constants (SCCs) used for each aqueous Pd species contained in the TDB were obtained using the respective FRCs, along with the formation reactions outlined in Ref. [11]. For metal-binding hydroxyl surface species that bind to strong sites, the SCCs ($\log^{S}K_I$ and $\log^{S}K_M$, where I represents illite, and M represents montmorillonite) were calculated from the hydrolysis constants ($\log^{OH}K$) in the TDB using the LFERs developed by Bradbury and Baeyens [12–14] for both illite and montmorillonite, shown in Eqs. (2) and (3), respectively.

$$\mathrm{Log}^{S}K_I = 7.9 \pm 0.4 + (0.83 \pm 0.02)\mathrm{Log}^{OH}K \quad (2)$$

$$\mathrm{Log}^{S}K_M = 8.1 \pm 0.3 + (0.90 \pm 0.02)\mathrm{Log}^{OH}K \quad (3)$$

For ternary surface species, the relationship presented in Fein [32] for organic ligands in ternary complexes was analogously followed for inorganic ligands in ternary complexes. The linear correlation between the logarithm of the SCC for the ternary complex (Log K_T) and the sum of the logarithm of the SCC for the ligand-surface complex (Log $K_{S\text{-}L}$), and the logarithm of the FRC for the metal-ligand aqueous complex (Log $K_{M\text{-}L\ (aq)}$) shown in Eq. (4) is referred to in this paper as the "Fein correlation" [32].

$$\mathrm{Log}K_T = 0.992\left(\mathrm{Log}K_{S-L} + \mathrm{Log}K_{M-L\ (aq)}\right) \quad (4)$$

Sorption of chlorine directly onto shale and MX-80 was not detected by Vilks [4], so the inorganic ligand SCCs (Log $K_{S\text{-}L}$) for both illite and MX-80 were taken to be zero. This reduces Eq. (4) to Eq.

(5), where the ternary SCC (Log K_T), is equal to the metal-ligand aqueous FRC (Log $K_{M\text{-}L\ (aq)}$).

$$\mathrm{Log}K_T \approx \mathrm{Log}K_{M-L\ (aq)} \tag{5}$$

Eq. (5) allowed us to use the FRCs for the various Pd species in the TDB as the initial SCC values for the related ternary surface species. These initial guesses for both the metal binding and ternary SCCs of the various Pd species are summarized in Table 2, where the general symbols for SCCs for illite ($\mathrm{Log}^S K_I$) and montmorillonite ($\mathrm{Log}^S K_M$) have been used for the ternary complexes instead of Log K_T.

The initial guess for the cation exchange (CE) constant of the primary Pd exchange species (X_2Pd) had to be calculated due to a lack of proposed values in the existing literature. Since the Gaines-Thomas convention [33] is the computational method used in PHREEQC [34], it was followed in calculating the selectivity coefficient (K_c) for an association reaction of the type shown in Eq. (6) using Eq. (7).

$$z_B A^{Z_A} - clay + z_A B^{Z_B} \leftrightarrow z_A B^{Z_B} - clay + z_B A^{Z_A} \tag{6}$$

$$ {}^{B}_{A}K_c = \left({}^{B}R_d\right)^{Z_A} \cdot \frac{(z_B)}{(CEC)^{Z_A}} \cdot [A]^{Z_B} \cdot \frac{(\gamma_A)^{Z_B}}{(\gamma_B)^{Z_A}} \tag{7}$$

In this, ${}^{B}R_d$ is the distribution coefficient for metal B, as shown in Eq. (6) [12], CEC is the cation exchange capacity of the soil, z is the charge of the ion, γ is the aqueous phase activity coefficient, and [A] is the concentration of species A. Eqs. (8) and (9) are obtained through applying Eqs. (6) and (7) to a Pd solution with a sodium cation-rich background electrolyte.

$$2Na^{+} - clay + Pd^{2+} \leftrightarrow Pd^{2+} - clay + 2Na^{+} \tag{8}$$

$$ {}^{Pd}_{Na}K_c = \left({}^{Pd}R_d\right) \cdot \frac{2}{(CEC)} \cdot [Na^{+}]^2 \cdot \frac{(\gamma_{Na})^2}{(\gamma_{Pd})} \tag{9}$$

R_d values used for calculating the Pd selectivity coefficients were from the experimental results obtained in this work. The Na concentration, activity coefficient, and Pd activity coefficient were obtained from the PHREEQC output file of the sorption model without the CE component of the model.

Initial guesses for the SCCs and the CE constants were modelled and plotted with the experimental R_d values obtained in this work (not shown here). CE constants were then optimized to fit the experimental data in regions of IS and pH_c where that sorption mechanism dominates: low IS and low pH_c. Once optimized, the CE constants were then fixed while the SCCs were optimized individually, starting with the hydroxyl species, in order to obtain the best fit to the experimental data. The SCCs for the ternary species could not be modified independently from the FRCs contained in the TDB being used, in accordance with the relationship developed in Eq. (5). If the ternary SCCs required optimization, they were adjusted in conjunction with the FRC of the corresponding aqueous species within the error range stated in the TDB.

Table 2
Initial SCCs for Pd(II) sorption model.

Surface Complexation Reaction	$\mathrm{Log}^S K_I$	$\mathrm{Log}^S K_M$
Metal Binding:		
$S{-}OH + Pd^{2+} \leftrightarrow S{-}OPd^{+} + H^{+}$	6.36	6.43
$S{-}OH + Pd^{2+} + H_2O \leftrightarrow S{-}OPdOH + 2H^{+}$	5.00	4.96
$S{-}OH + Pd^{2+} + 2H_2O \leftrightarrow S{-}OPd(OH)_2^{-} + 3H^{+}$	−4.95	−5.83
$S{-}OH + Pd^{2+} + 3H_2O \leftrightarrow S{-}OPd(OH)_3^{2-} + 4H^{+}$	−16.47	−18.32
Ternary:		
$S{-}OH + Pd^{2+} + Cl^{-} \leftrightarrow S{-}OPdCl + H^{+}$	5.00	5.00
$S{-}OH + Pd^{2+} + 2Cl^{-} \leftrightarrow S{-}OPdCl_2^{-} + H^{+}$	8.42	8.42
$S{-}OH + Pd^{2+} + 3Cl^{-} \leftrightarrow S{-}OPdCl_3^{2-} + H^{+}$	10.93	10.93
$S{-}OH + Pd^{2+} + 4Cl^{-} \leftrightarrow S{-}OPdCl_4^{3-} + H^{+}$	13.05	13.05
$S{-}OH + Pd^{2+} + 3Cl^{-} + H_2O \leftrightarrow S{-}OPdCl_3OH^{3-} + 2H^{+}$	3.77	3.77

4. Results & discussion

4.1. Sorption kinetics

Sorption of Pd was found to increase between 2 and 7 days in contact with each of the three sorbents tested, but remained constant between 7 and 14 days as shown in Figs. 1–3 for illite, MX-80, and shale, respectively. Therefore, a sorption duration of at least 7 days is required to ensure that equilibrium is reached. This duration was doubled to 14 days when selecting the sorption duration for all experimental conditions. Although this sorption duration contrasts the 30-day sorption duration used in previous Pd sorption experiments [5], we were able to demonstrate that 14 days is sufficient in most cases. However, it is possible that it takes longer than 14 days for Pd sorption to reach equilibrium in 1.0 M Na–Ca–Cl conditions.

4.2. Ionic strength dependence

The IS dependence of the R_d values for Pd sorption onto the three sorbents is illustrated in Fig. 4. Overall, the R_d values decreased with increasing IS. This decrease in Pd sorption is likely due to increased competing sorption as the background electrolyte concentration increases. Of the solids tested, shale exhibited the largest decrease in sorption across the IS range.

There is scatter present in the data for all solids tested, with MX-80 having the most scattered results. Of the solids tested, only MX-80 showed a definitive minimum in sorption with increasing IS, which occurred between IS of 3.0–4.0 M. Previous analysis of MX-80 clay with XRD and XRF techniques has shown that there can be variability in composition of the clay due to sample preparation [35]. This could account for a small amount of the scatter in the data; however, heterogeneity of solid samples would not produce the minimum that was observed. Another thought was that differing pH of the samples could have caused the irregular sorption behavior. However, inspection of the pH values for the MX-80 samples showed that they were within half a value of each other, which would not lead to a significant difference in sorption at a pH of around 6. Furthermore, these results were reproduced in the pH dependency experiments for MX-80, shown in Fig. 6. Thus, the cause of the irregular sorption behavior could not be determined at present and should further be investigated in the future.

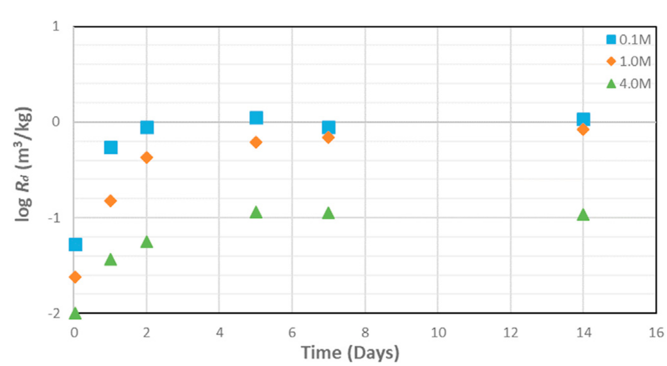

Fig. 1. Pd sorption kinetics over 14 days on illite in 0.1, 1.0, and 4.0 M ionic strength Na–Ca–Cl solutions.

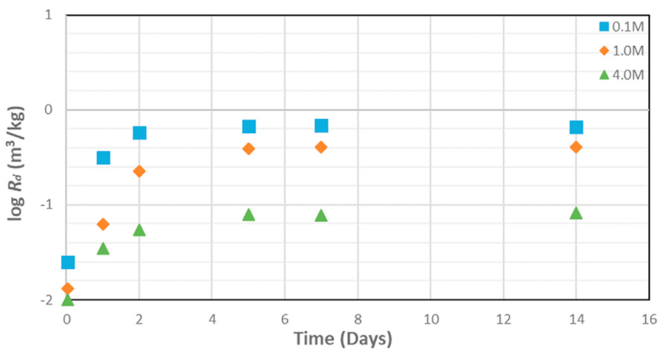

Fig. 2. Pd sorption kinetics over 14 days on MX-80 in 0.1, 1.0, and 4.0 M ionic strength Na–Ca–Cl solutions.

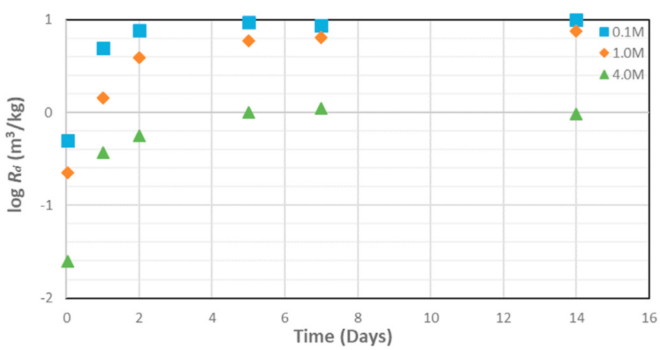

Fig. 3. Pd sorption kinetics over 14 days on shale in 0.1, 1.0, and 4.0 M ionic strength Na–Ca–Cl solutions.

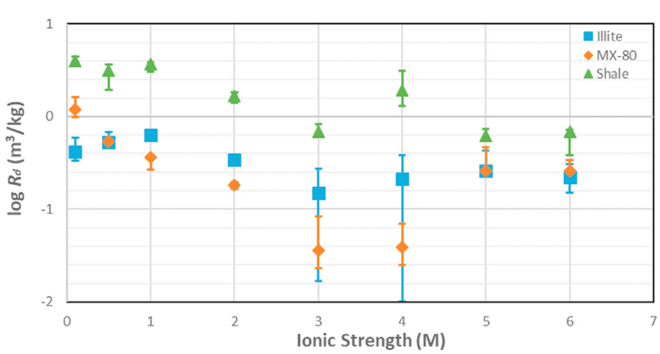

Fig. 4. Ionic strength dependence of Pd R_d value for illite, MX-80, and shale.

4.3. pH_c dependence

The pH_c dependence of the R_d values of Pd sorption onto illite, MX-80, and shale are shown in Figs. 5–7, respectively. For the Pd sorption onto illite (Fig. 5) and MX-80 (Fig. 6), the R_d value increased with pH_c, reached a maximum, then slightly decreased before becoming independent of pH_c at IS = 0.01 M. For IS $\geq$ 0.1 M, the R_d value increased with pH_c and then became independent of pH_c. For the Pd sorption onto shale (Fig. 7), the R_d value appears to be relatively independent of pH_c at IS = 0.1, 1.0, and 6.0 M, but the trend for IS = 4.0 M was different. This will be discussed with the future work at the end of this section.

Figs. 5 and 6 show the fitted results of the 2SPNE SC/CE model, in addition to the experimental data. As mentioned previously, the lack of Pd^{2+} Pitzer parameters forces the use of the SIT method, which limits modelling to IS $\leq$ 4.0 M. For both figures, some experimental data is not shown due to the R_d values being too small to measure, which indicates that there is zero, or nearly zero, sorption of Pd^{2+} at these pH_c and IS values. These data points occurred in the low pH region (pH_c of 3–5) as IS increased. The R_d data that is indicative of zero sorption was also excluded from the experimental data that the model replicates. The optimized values of the SCCs and CECs for illite and MX-80 are listed in Table 3. Solid surface and solution speciation plots for all IS modelled are shown in the Supplemental Information section (Figs. A2 – A4 for illite, A5 – A7 for MX-80, and A8 – A10 for IS = 0.01, 0.1, and 4.0 M). Given the uncertainty in the equilibrium of the 1.0 M data, a model for 1.0 M conditions was not attempted. As this is currently the first investigation into the sorption of Pd^{2+} onto illite and MX-80 across a wide pH range, with a broad IS range, these results and corresponding SCM are valuable to the Canadian DGR project.

The discrepancies between the model and the experimental data present notable areas to focus research efforts to properly quantify Pd^{2+} sorption onto illite and MX-80. One of these areas is the speciation being considered in the model. It was found that Pd^{2+} sorption could largely be accounted for with the formation of the S–OPdOH, S–OPd$(OH)_2^-$, and S–OPdCl_4^{3-} surface species, and the S–O_2Pd cation exchange species with 2 Na^+ for both sorbents, with the additional S–OPd^+ surface species for MX-80. Five possible ternary sorption reactions were originally included in the model, shown in Table 2, but only one reaction (S–OH + Pd^{2+} + 4Cl^- $\leftrightarrow$ S–OPdCl_4^{3-} + H^+) was found to contribute to the sorption, even in Na–Ca–Cl solutions with high IS. For illite at IS = 0.01, 0.1, and 4.0 M, the simulation results were consistent with the experimental results, except for the 0.1 M data at a pH of 5.1 where the model under predicted sorption. For MX-80 at IS = 0.01 M, model fitting results were consistent with the experimental results, but at IS = 0.1 M and 4.0 M the model could not be fitted to the R_d values in the low pH region (pH_c = 3–5) and in the high pH region (pH_c = 8–9), respectively; there was under prediction of sorption in the low pH region, while there was over prediction in the high pH region. Due to the model failing to replicate the experimental data in all cases, the speciation chosen to represent Pd^{2+} sorption may not be complete. Future experimental and simulation work will allow for this SCM to be re-evaluated and improved upon.

Another important aspect to consider is the divalent cationic nature of Pd^{2+} and Ca^{2+}, coupled with the high concentration of Ca^{2+} present in all solutions. The competing nature of these two divalent ions may require implementation of an electrostatic model. However, previously reported 2SPNE SC/CE model results with these identical solutions and sorbents (albeit different sorbing elements) have been able to replicate experimental data accurately without considering the electrostatics of Ca^{2+} sorption [16]. It is believed that further experimental and simulation work is needed to fully understand the competing sorption effects between these two ions.

As highlighted in Table 3, it was also found that the optimized metal-binding SCC values were mostly outside of the range of values estimated by the LFER (Table 4). Since the LFER uses FRCs of aqueous species to estimate the corresponding SCCs, this could indicate that the thermodynamic data for Pd^{2+} needs to be updated in the TDBs. However, as mentioned previously, electrostatic effects could play an important role in the sorption of Pd onto illite and MX-80 and a non-electrostatic model may not be adequate. Therefore, we cannot say with certainty that the thermodynamic data for Pd^{2+} needs to be updated, only that it is a possibility.

Looking at the shale data in Fig. 7, the trend for 4.0 M was different than for the other IS; instead of being relatively constant across the pH range, there was a peak around a pH_c of 6.5. Sorption in the 4.0 M case was also lower than that in the 6.0 M case in the low pH region (pH_c = 5–6) instead of being higher or about the

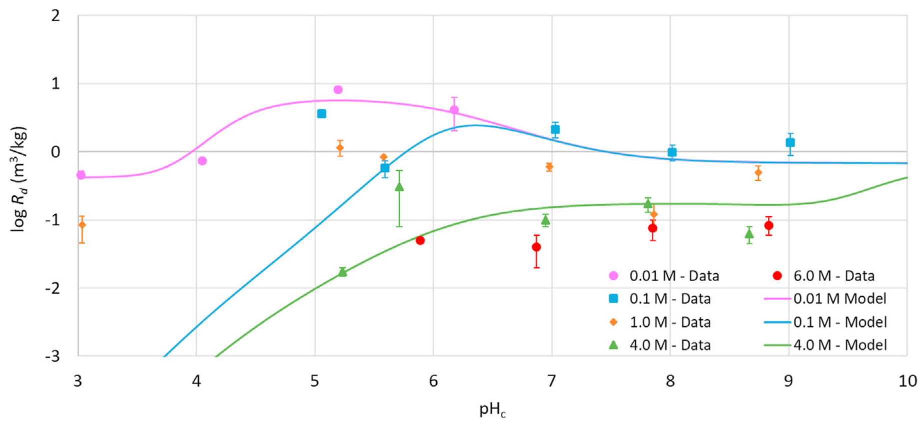

Fig. 5. pH$_c$ dependence of Pd R_d value for illite at IS = 0.01, 0.1, 1.0, 4.0, and 6.0 M.

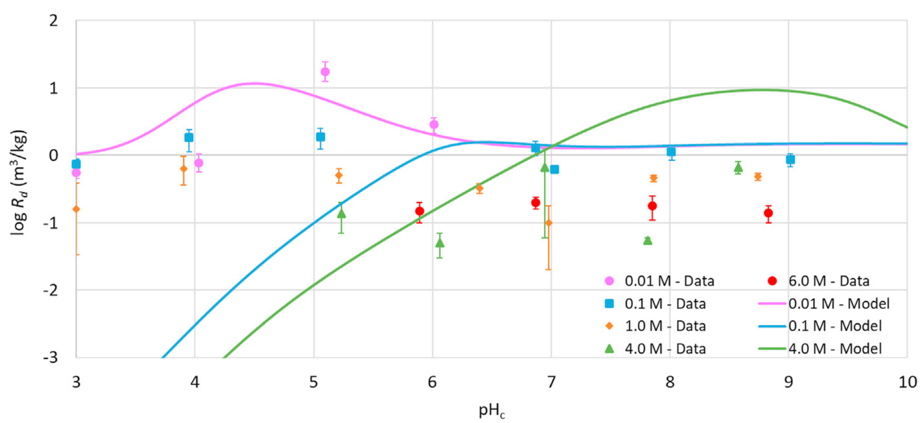

Fig. 6. pH$_c$ dependence of Pd R_d value for MX-80 at IS = 0.01, 0.1, 1.0, 4.0, and 6.0 M.

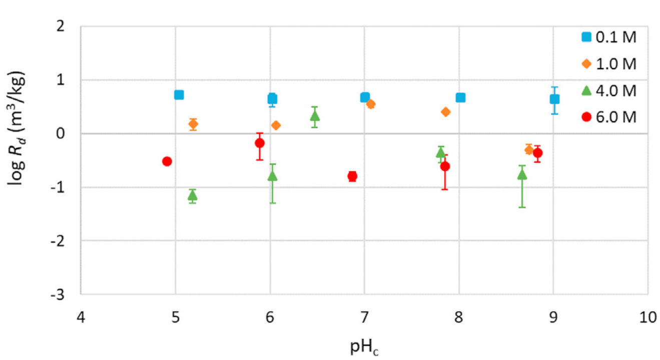

Fig. 7. pH$_c$ dependence of Pd R_d value for shale at IS = 0.1, 1.0, 4.0, and 6.0 M.

same. Since shale is composed of many constituent minerals, the sorption process is more complex than for illite and MX-80. To gain a better understanding of the sorption process onto shale for Pd^{2+}, sorption of Pd^{2+} should be investigated onto both the dominant and minor constituent minerals of shale as minor constituents have previously been shown to contribute to sorption [19]. This experimental data could then be used in the development of a SCM for shale to obtain a more detailed understanding of the sorption process.

5. Conclusions

This is the first research systematically studying the sorption behaviour of Pd in Na–Ca–Cl solutions with high IS. The sorption kinetics and the ionic strength and pH$_c$ dependence of Pd sorption for illite (Silver Hill), MX-80 bentonite, and Queenston shale in Na–Ca–Cl solutions were measured.

Table 3
Optimized surface complexation and CE constants used for Pd(II) sorption modelling.

Surface Complexation Reaction	$Log^S K_I$	$Log^S K_M$
Metal Binding:		
S–OH + Pd^{2+} ↔ S–OPd$^+$ + H^+	–	**8.2 ± 0.2**
S–OH + Pd^{2+} + H_2O ↔ S–OPdOH + 2H^+	**3.2 ± 0.2**	**2.3 ± 0.2**
S–OH + Pd^{2+} + 2H_2O ↔ S–OPd(OH)$_2^-$ + 3H^+	**−4.0 ± 0.2**	−5.5 ± 0.2
Ternary:		
S–OH + Pd^{2+} + 4Cl^- ↔ S–OPdCl$_4^{3-}$ + H^+	13.05 ± 0.2	13.05 ± 0.2
Ion-Exchange:		
2S–ONa + Pd^{2+} ↔ S–O_2Pd + 2Na^+	6.75 ± 0.2	5.90 ± 0.2

*Reaction constants bold highlighted fall outside of the range of the LFER.

Table 4
Range of SCCs allowed for LFER [12–14] based on FRCs for Pd(II) sorption [26].

Surface Complexation Reaction	$Log^S K_I$	$Log^S K_M$
S–OH + Pd^{2+} ↔ S–OPd$^+$ + H^+	5.93–6.80	6.10–6.77
S–OH + Pd^{2+} + H_2O ↔ S–OPdOH + 2H^+	4.53–5.47	4.59–5.33
S–OH + Pd^{2+} + 2H_2O ↔ S–OPd(OH)$_2^-$ + 3H^+	−5.66–−4.24	−6.44–−5.22

Pd sorption onto illite, MX-80, and shale was found to reach equilibrium within 7 days, except for 1.0 M conditions. The Pd R_d values were obtained across large portions of the pH spectrum in solutions of varying IS for all three sorbents. By fitting of 2SPNE SC/CE model to the pH_c dependence of experimentally derived R_d values for illite and MX-80, it was found that Pd sorption could largely be accounted for with the formation of the S–OPdOH, $S{-}OPd(OH)_2^-$, $S{-}OPdCl_4^{3-}$ surface species, the $S{-}O_2Pd$ exchange species with $2Na^+$ for both sorbents, and the additional $S{-}OPd^+$ surface species for MX-80. The optimized values of SCCs and CE constants were estimated, but the optimized SCC values were found to fall outside the ranges of the values estimated by the LFER, with the exception of the $S{-}OPd(OH)_2^-$ surface species for MX-80. There are still discrepancies between the predicted R_d values by the 2SPNE SC/CE model and those measured. The reason for these discrepancies could not be identified, but possibilities include competing sorption effects of the divalent Pd^{2+} and Ca^{2+} ions, a need to update and improve the speciation of Pd^{2+} being considered in the SCM, or needing to implement an electrostatic model.

Declaration of competing interest

The authors declare that they have no known competing financial interests or personal relationships that could have appeared to influence the work reported in this paper.

Acknowledgements

The authors would like to thank Dr. Tammy Yang (the Nuclear Waste Management Organization of Canada) for her helpful comments on the sorption experiments. The authors wish to acknowledge Drs. Yoshihisa Iida and Tetsuji Yamaguchi (Japan Atomic Energy Agency), Dr. Takumi Saito (the University of Tokyo), and Dr. Peter Vilks (Canada Nuclear Laboratory) for the fruitful discussion on Pd sorption experiments and modelling. The authors would also like to thank Dr. Naoki Sugiyama of Agilent Technologies for helpful discussions on Pd measurement and improvement of the detection limit of Pd by ICP-MS in saline solutions.

Appendix A. Supplementary data

Supplementary data to this article can be found online at https://doi.org/10.1016/j.net.2020.09.001.

References

[1] J. Noronha, Deep Geological Repository Conceptual Design Report, Crystalline/Sedimentary Rock Environment, Technical Report, Nuclear Waste Management Organization, May 2016. APM-REP-00440-0015 R001.
[2] Nuclear Fuel Waste Act, Statute of Canada, 2002 c. 23.
[3] P. Vilks, T. Yang, Sorption of Selected Radionuclides on Sedimentary Rocks in Saline Conditions - Updated Sorption Values, Technical Report, Nuclear Waste Management Organization, 2018. NWMO-TR-2018-03.
[4] P. Vilks, N.H. Miller, Sorption Studies with Sedimentary Rocks under Saline Conditions, Technical Report, Nuclear Waste Management Organization, 2014. NWMO-TR-2013-22.
[5] T.L. Rakitskaya, V.O. Vasylechko, T.A. Kiose, G.M. Dzhyga, G.V. Gryshchouk, V.Y. Volkova, Some features of Pd(II) and Cu(II) adsorption on bentonite, Adsorpt. Sci. Technol. 35 (5–6) (2017) 482–489.
[6] S. Shen, T. Pan, X. Liu, L. Yuan, Y. Zhang, J. Wang, Z. Guo, Adsorption of Pd(II) complexes from chloride solutions obtained by leaching chlorinated spent automotive catalysts on ion exchange resin Diaion WA21J, J. Colloid Interface Sci. 345 (2010) 12–18.
[7] S. Cataldo, N. Muratore, S. Orecchio, A. Pettignano, Enhancement of adsorption ability of calcium alginate gel beads towards Pd(II) ion. A kinetic and equilibrium study on hybrid Laponite and Montmorillonite–alginate gel beads, Appl. Clay Sci. 118 (2015) 162–170.
[8] T. Kobayashil, T. Sasaki, K. Ueda, A. Kitamura, Sorption behavior of nickel and palladium in the presence of $NH_3(aq)/NH_4^+$, Mater. Res. Soc. Symp. Proc. 1518 (2013) 231–236.
[9] Y. Tachi, T. Shibutani, H. Sato, M. Shibata, Sorption and Diffusion Behavior of Palladium in Bentonite, Granodiorite and Tuff, Technical Report, Japan Nuclear Cycle Development Institute, 1999.
[10] D.L. Parkhurst, C. Appelo, Description of input and examples for PHREEQC version 3 – a computer program for speciation, batch-reaction, one-dimensional transport, and inverse geochemical calculations, U.S. Geol. Surv. Tech. Methods (2013) book 6, ch. A43.
[11] W. Stumm, J.J. Morgan, Aquatic Chemistry: Chemical Equilibria and Rates in Natural Waters, third ed., John Wiley & Sons, Inc., New York, 1996.
[12] M.H. Bradbury, B. Baeyens, Modelling the sorption of Mn(II), Co(II), Ni(II), Zn(II), Cd(II), Eu(III), Am(III), Sn(IV), Th(IV), Np(V) and U(VI) on montmorillonite: linear free energy relationships and estimates of surface binding constants for some selected heavy metals and actinides, Geochem. Cosmochim. Acta 69 (4) (2005) 875–892.
[13] M.H. Bradbury, B. Baeyens, Sorption modelling on illite. Part I: titration measurement and the sorption of Ni, Co, Eu, and Sn, Geochem. Cosmochim. Acta 73 (4) (2009) 990–1003.
[14] M.H. Bradbury, B. Baeyens, Sorption modelling on illite. Part II: actinide sorption and linear free energy relationships, Geochem. Cosmochim. Acta 73 (4) (2009) 1004–1013.
[15] R. Marsac, N.I. Banik, J. Lützenkirchen, C.M. Marquardt, K. Dardenne, D. Schild, J. Rothe, A. Diascorn, T. Kupcik, T. Schafer, H. Geckeis, Neptunium redox speciation at the Illite surface, Geochem. Cosmochim. Acta 152 (2015) 39–51.
[16] S. Nagasaki, J. Riddoch, T.S. Saito, J. Goguen, A. Walker, T. Yang, Sorption behaviour of Np(IV) on illite, shale and MX-80 in high ionic strength solutions, J. Radioanal. Nucl. Chem. 313 (2017) 1–11.
[17] D. Soltermann, B. Baeyens, M.H. Bradbury, M.M. Fernandes, Fe(II) uptake on natural montmorillonites. II. Surface complexation modeling, Environ. Sci. Technol. 48 (15) (2014) 8698–8705.
[18] T. Sasaki, K. Ueda, T. Saito, N. Aoyagi, T. Kobayashi, I. Takagi, T. Kimura, Y. Tachi, Sorption of Eu^{3+} on Na-montmorillonite studied by time-resolved laser fluorescence spectroscopy and surface complexation modeling, J. Nucl. Sci. Technol. 53 (4) (2016) 592–601.
[19] S. Nagasaki, Sorption Properties of Np on Shale, Illite and Bentonite under Saline, Oxidizing and Reducing Conditions, Technical Report, Nuclear Waste Management Organization, January 2018. NWMO-TR-2018-02.
[20] T. Fanghänel, V. Neck, J.I. Kim, The ion product of H_2O, dissociation constants of H_2CO_3 and pitzer parameters in the system $Na^+/H^+/OH^-/HCO_3^-/CO_3^{2-}/ClO_4^-/H_2O$ at 25°C, J. Solut. Chem. 25 (1996) 327–343.
[21] M. Altmaier, V. Metz, V. Neck, R. Müller, T. Fanghänel, Solid-liquid equilibria of $Mg(OH)_2$(cr) and $Mg_2(OH)_3Cl{\cdot}4H_2O$(cr) in the system Mg-Na-H-OH-Cl-H_2O at 25°C, Geochem. Cosmochim. Acta 67 (19) (2003) 3595–3601.
[22] M. Altmaier, V. Neck, T. Fanghänel, Solubility of Zr(IV), Th(IV) and Pu(IV) hydrous oxides in $CaCl_2$ solutions and the formation of ternary Ca-M(IV)-OH complexes, Radiochim. Acta 96 (9–11) (2009) 541–550.
[23] S. Nagasaki, T. Saito, T.T. Yang, Sorption behavior of Np(V) on illite, shale and MX-80 in high ionic strength solutions, J. Radioanal. Nucl. Chem. 308 (1) (2016) 143–153.
[24] N. Sugiyama, Agilent Technologies, Private Communication, 2013.
[25] I. Grenthe, A. Plyasunov, On the use of semiempirical electrolyte theories for the modeling of solution chemical data, Pure Appl. Chem. 69 (5) (1997) 951–958.
[26] Thermodynamic database, Japan atomic energy agency, TDB Ver. 2014/03, https://migrationdb.jaea.go.jp/cgi-bin/db_menu.cgi?title=TDB&ej=1, June 2014.
[27] PHREEQC (version 3)-A computer program for speciation, batch-reaction, one-dimensional transport, and inverse geochemical calculations, United States Geol. Surv., https://wwwbrr.cr.usgs.gov/projects/GWC_coupled/phreeqc/.
[28] L. Charlet, C. Tournassat, Fe(II)–Na(I)–Ca(II) cation exchange on montmorillonite in chloride medium: evidence for preferential clay adsorption of chloride – metal ion pairs in seawater, Aquat. Geochem. 11 (2005) 115–137.
[29] S. Pivovarov, Physico-chemical modeling of heavy metals (Cd, Zn, Cu) in natural environments, Encycloped. Surface Colloid Sci. 5 (2004) 468–492, 2004 Update Supplement.
[30] F.P. Bertetti, Determination of Sorption Properties for Sedimentary Rocks under Saline, Reducing Conditions – Key Radionuclides, Technical Report, Nuclear Waste Management Organization, June 2016. NWMO-TR-2016-08.
[31] M. Villa-Alfageme, S. Hurtado, M.A. Castro, S.E. Mrabet, M.M. Orta, M.C. Pazos, M.D. Alba, Quantification and comparison of the reaction properties of FEBEX and MX-80 clays with saponite: europium immobilisers under subcritical conditions, Appl. Clay Sci. 101 (2014) 10–15.
[32] J.B. Fein, The Effects of Ternary Surface Complexes on the Adsorption of Metal Cations and Organic Acids onto Mineral Surfaces, Water-Rock Interactions, Ore Deposits, and Environmental Geochemistry: A Tribute to David A. Crerar, vol. 7, Geochemical Society, Special Publication, 2002, pp. 365–378.
[33] C.A.J. Appelo, D. Postma, Geochemistry, Groundwater and Pollution, second ed., 2005, p. 252.
[34] D.L. Parkhurst, C.A.J. Appelo, User's Guide to PHREEQC (Version 2) (Equations on Which the Program Is Based), Technical Report, U.S. Department of the Interior, U.S. Geological Survey, 1999. Water-Resources Investigations Report 99-4259.
[35] D. Dixon, A. Man, S. Rimal, J. Stone, G. Siemens, Bentonite Seal Properties in Saline Water, December 2018. NWMO TR-2018-20.